2015 NDIA GROUND VEHICLE SYSTEMS ENGINEERING AND TECHNOLOGY SYMPOSIUM
MODELING & SIMULATION, TESTING AND VALIDATION (MSTV) TECHNICAL SESSION
AUGUST 4-6, 2015 - NOVI, MICHIGAN

METHODOLOGY DEVELOPMENT OF COMPUTATIONALLY-EFFICIENT FULL VEHICLE SIMULATIONS FOR THE ENTIRE BLAST EVENT

Mohan Parthasarathy, PhD
Philip G. Kosarek
Julien Santini
ProductDesign Inc., Altair
Troy, MI

Ravi Thyagarajan, PhD
Deputy Chief Scientist,
Office of the Chief Scientist
US Army RDECOM-TARDEC
Warren, MI

ABSTRACT

Improvised Explosive Devices (IEDs) and mines pose significant threat to military ground vehicles and soldiers in the field. Due to the severity of the forces exerted by a blast, ground vehicles may undergo multiple sub-events subsequent to an explosion, including local structural deformation of the floor, gravity flight and slam-down. The current method of choice to simulate the effect of a shallow-buried IED or mine on a Lagrangian vehicle model, is a fluid-structure interaction with the environment modelled with an Eulerian formulation (explosive, ground, air) [1]. This method, also called Arbitrary Lagrangian-Eulerian (ALE), is more expensive and involved than pure structural methods (usually pressure loads applied to the vehicle surface). However, it allows for taking into account the effect of the shape, type and size of the charge and the soil characteristics on the impulse transmitted to the vehicle. Three approaches are proposed to reduce the analytical simulation time while maintaining the highest level of accuracy throughout the full blast and subsequent sub-events. The tradeoffs between the approaches are detailed in this paper.

INTRODUCTION

Improvised Explosive Devices (IEDs) and mines pose significant threat to military ground vehicles and soldiers in the field. Vehicles may undergo multiple sub-events like local structural deformation of the floor, blast-off and slam-down. To understand injuries sustained by soldiers, it is imperative to analyze impact of each sub-event on soldier injuries. Using traditional finite element analysis techniques [1-6] to evaluate an entire event is computationally very expensive, requiring several days of CPU time. So there is considerable impetus to speed up the time taken for these simulations, and significant research has been conducted in this area [7-11].

The goal of this project was to develop a cost-effective methodology that allows simulating a full blast event (blast-off, gravity flight and return-to-ground) accurately and efficiently.

MODEL DESCRIPTION

The conceptual, generic vehicle used for the blast methodology development study is comprised of 5 major assemblies (Cab, chassis, suspension, seat and driver dummy). The mass of the vehicle is approximately 20,000 lb (9,000 kg). Figure 1 below shows the overall dimensions of the vehicle for this study.

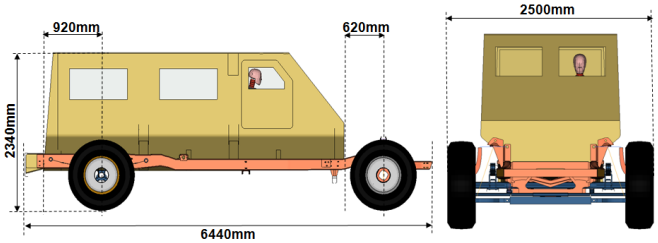

Figure 1: Vehicle Dimensions

CAB DETAILS

The TARDEC Generic Hull is used as the Cab and is comprised of 230,842 shell elements shown in Figure 2. Many unclassified studies from past researchers have utilized fictitious vehicle geometry due to the unavailability of realistic information. Due to the sensitive nature of the work performed by the Department of Defense, data

generated from testing military vehicles is usually classified, making it difficult to share data in the public domain.

In order to increase the operational relevance of studies performed by the wider scientific community, the US Army Tank Automotive Research, Development and Engineering Center (RDECOM-TARDEC) recently fabricated a generic vehicle hull, aka TARDEC Generic Hull, shown in Figure 2, with the intent to:

- Subject it to an underbody mine blast test
- Share the data publicly
- Evaluate blast mitigation technologies

This effort has been described in detail [12, 13] and continues to be analyzed and refined for industry consumption. This paper does not serve as the source for dissemination of these findings of the generic vehicle hull but does utilize a similar test configuration and vehicle geometry.

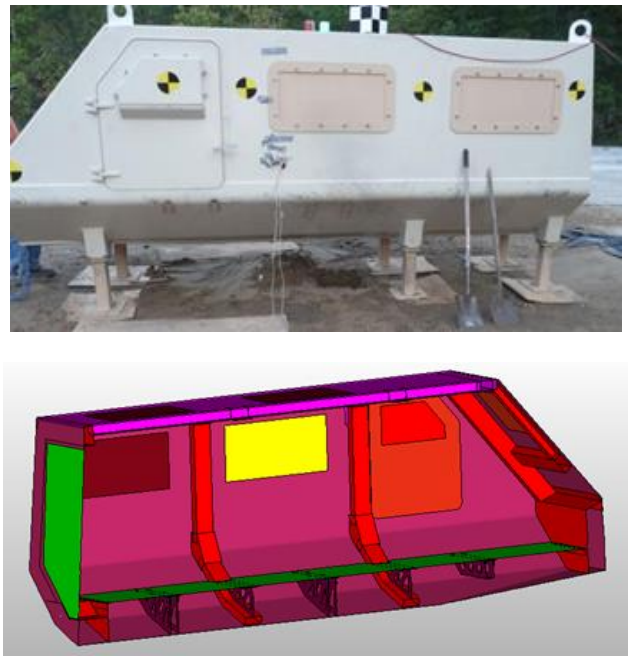

Figure 2: TARDEC Generic Hull (top) used for the Cab Model in this study (bottom)

The connection between different components of the Cab is represented by nodal rigid bodies and spotwelds. Elastic-plastic material laws without strain rate effects are used for the metallic parts (hull, floor, frames, cross members, etc.) and a purely elastic behavior is assumed for the window panes and windshield.

CHASSIS & SUSPENSION DETAILS

The chassis for this vehicle was generated by morphing the chassis of a High Mobility Multipurpose Wheeled Vehicle (HMMWV). The suspension was created from suspension systems used on small trucks (Ford F150, Dodge Ram, etc.). The chassis and suspension structure are comprised of 73,947 elements. The chassis is connected to the Cab with rigid elements at discrete locations as shown in Figure 3.

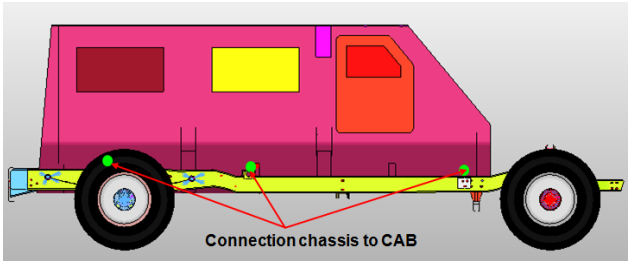

Figure 3: Connection of Chassis to Cab

The suspension system, shown in Figure 4, is connected to the chassis with rigid elements and kinematic joints to allow articulation of the suspension. The coil springs and shock absorber are modeled with discrete beam elements with a function defining the evolution of the force versus deflection. The leaf springs are explicitly modelled with shell elements.

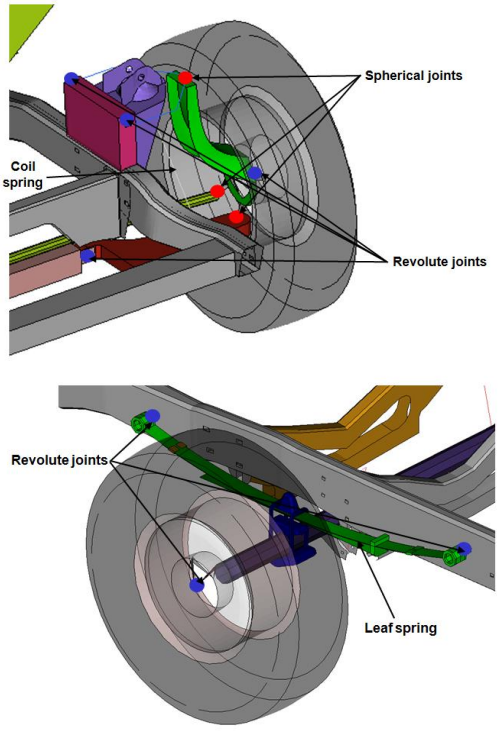

Figure 4: Front and Rear Suspension

SEAT & SAFETY DUMMY DETAILS

The Anthropomorphic Test Device (ATD) safety dummy used for the blast method development is known as the (H3_50TH_FAST.111130_V2.0) LSTC FAST 50th percentile dummy from LSTC Corporation [3], which is a simplified depiction of a typical Hybrid-III dummy. The ATD shown in Figure 5 was positioned with the eyes centered in the windshield. Force and acceleration responses from this ATD model can be used to assess accelerative injuries sustained by the occupant [14-16].

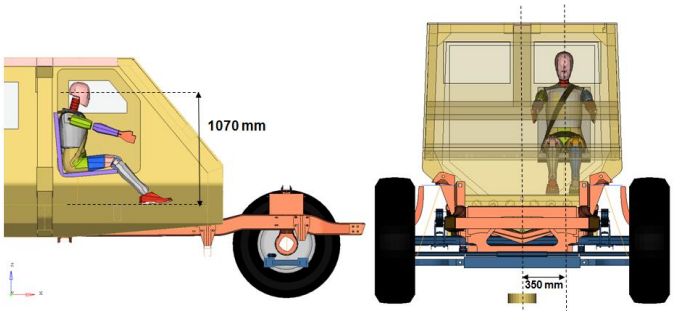

Figure 5: Hybrid 50th Percentile Position

A simplified seat with a stroking mechanism was created to support the ATD and a 3 point restraint system was generated to secure the dummy onto the seat during the event. This is shown in Figure 6. The seat is constrained to the Cab in all degrees of freedom except the vertical direction and connected to the Cab floor through the stroking mechanism with a rigid element.

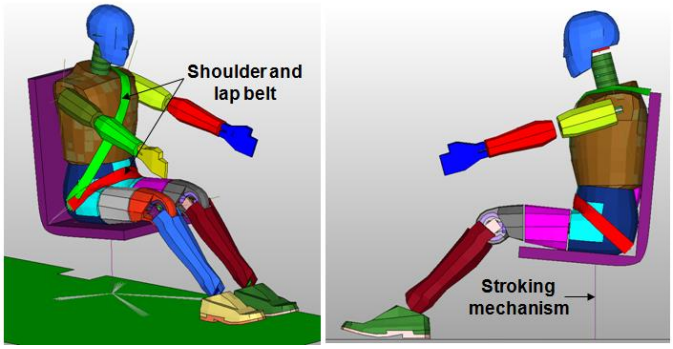

Figure 6: Seat and Restraint System

FLUID DESCRIPTION

The fluid domain (air, explosive, soil) is modeled using an Eulerian formulation with approximately 2.5 million 3D hexahedral elements. The element formulation 11 in LS-DYNA [3] is used (1 point ALE multi-material) and the average mesh size is equal to 35mm. Fluid domain dimensions are shown in Figure 7.

The material model used for the explosive is *MAT_HIGH_EXPLOSIVE_BURN. An equation of state (*EOS_JWL) is used to define the evolution of the pressure as a function of the relative volume and energy. The explosive is assumed to be TNT. Only very generic charge sizes (shown in Appendix 1) were used in this study.

The air is modeled with a polynomial equation of state with a null material to define the density and cut-off pressure. The soil is modeled using the Mie-Gruneisen equation of state and an elastic-plastic material law to define the yield surface.

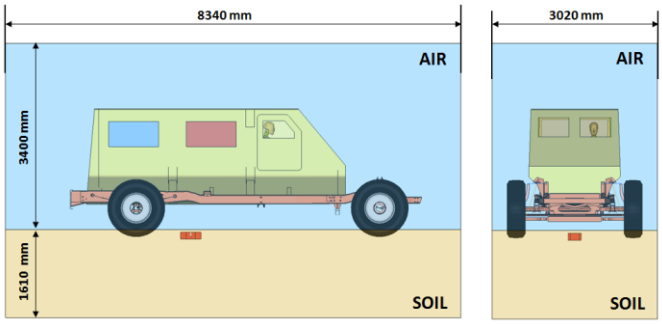

Figure 7: Fluid Domain Dimension

FLUID STRUCTURE INTERACTION DETAILS

To transmit the energy from the blast to the vehicle, the *CONSTRAINED_LAGRANGE_IN_SOLID coupling method in LS-DYNA is used.

The main advantages of this method are:

- The effect of the shape of the charge, stiffness of the soil, and the reflection of the shockwaves on the energy transmitted from the blast to the vehicle is directly taken into account.
- The structural mesh (vehicle) is not coincident with the fluid mesh (explosive, air and soil). Throughout the analysis there will not be any distortion of the fluid mesh. This greatly improves the stability of the simulation,
- Because there is no need to maintain connectivity between the fluid and structural mesh, design changes to the structure are easier than with direct coupling methods (coincident nodes between structure/fluid, fluid connected to the structure with tied contact).

The main drawbacks to this method are:

- The vehicle needs to be fully immersed in the fluid domain. The number of elements in the model can quickly become significantly large.
- The results are strongly dependent on the parameters used in the coupling that allows transmitting the energy from the fluid to the structure.

Figure 8 shows the overall setup used for the blast method development.

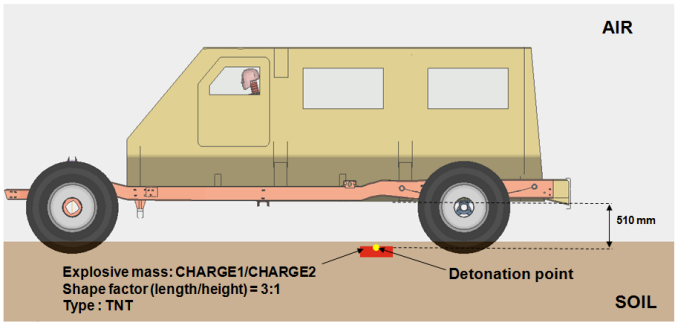

Figure 8: Blast Model Setup

EXPLOSIVE DESCRIPTION

In this study, two approaches were used to simulate the effect of an explosion on a vehicle.

1. Purely structural (*LOAD_BLAST) - Pressure time histories are applied to a group of elements on the vehicle underbody [18]. The amplitude and duration of the pressure pulse is computed based on analytical formulas (Brode, Henrych and Kinney-Graham) as a function of the mass of the explosive in TNT units and the distance between the centroid of the element and the center of the charge.
2. Fluid structure interaction (FSI) - The explosive, air, and the soil are explicitly modeled using an Eulerian formulation. Energy is transmitted from the blast to the vehicle using the fluid-structural coupling *CONSTRAINED_LAGRANGE_IN_SOLID.

AIR BLAST: SPHERICAL CHARGE

The effect of the free air burst of a spherical charge of size CHARGE1 (Appendix 1) onto the vehicle was simulated using methods (1) and (2) mentioned above. In order to improve the behavior of the coupling in method (2), it was necessary to define different multi-material groups and couplings on both sides of the Cab shell elements. Several iterations were made on the definition and parameters of the coupling in order to mitigate the leakage of the explosive and outside air into the vehicle.

Figure 9 shows a comparison of the stress on the hull at time = 0.8ms between the purely structural method (*LOAD_BLAST), the fluid-structure interaction (*CONSTRAINED_LAGRANGE_IN_SOLID) and the results from another commonly used non-linear explicit solver for impact simulations (RADIOSS, [4]) using a coupling similar to the one used in LS-DYNA.

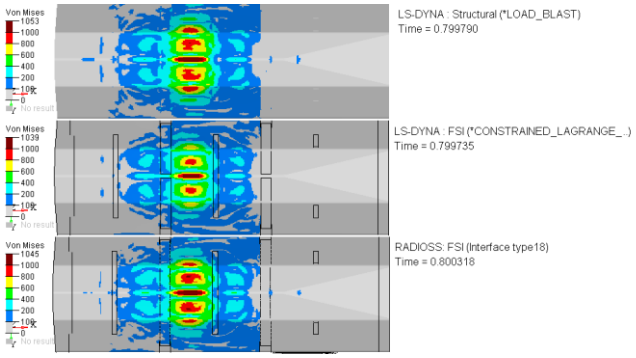

Figure 9: Free Air Burst – Spherical Charge, Hull Stress: Structural (top), LS-DYNA/FSI (mid), RADIOSS/FSI (bottom)

The results from RADIOSS FSI correlate well with that obtained using the structural method in LS-DYNA. The stress on the hull from the LS-DYNA FSI is similar in terms of distribution but lower in magnitude than those obtained with the purely structural method.

Figure 10 shows a comparison of the internal energy of the hull with different mesh densities for the fluid and advection methods (METH=1&3) with LS-DYNA FSI against a purely structural method LS-DYNA response and RADIOSS FSI response.

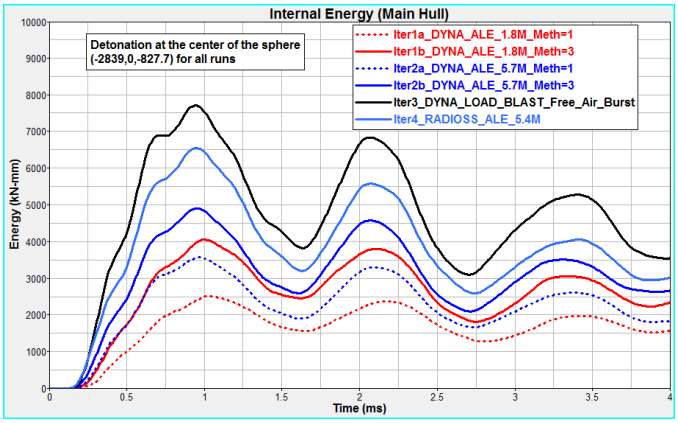

Figure 10: Free Air Burst – Spherical Charge, Hull Internal Energy

AIR BLAST: CYLINDRICAL CHARGE

The initial shape of the explosive charge can have an influence on the energy transmitted to the vehicle. Figure 11 and Figure 12 compare the results obtained using the LS-DYNA FSI method with a cylindrical charge of size CHARGE1 and an aspect ratio of 3:1 to those obtained with a spherical charge of the same size.

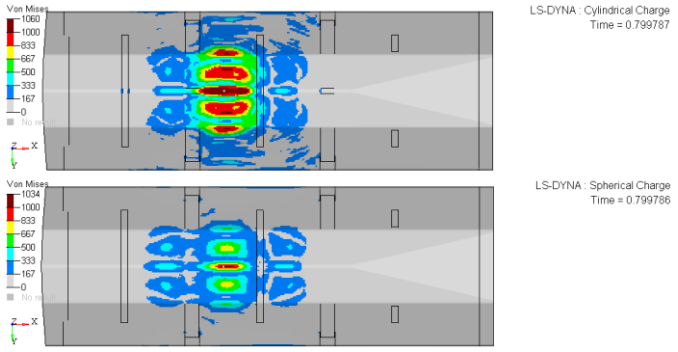

Figure 11: Free Air Burst –Hull Stress, Cylindrical Charge (top), Spherical Charge (bottom)

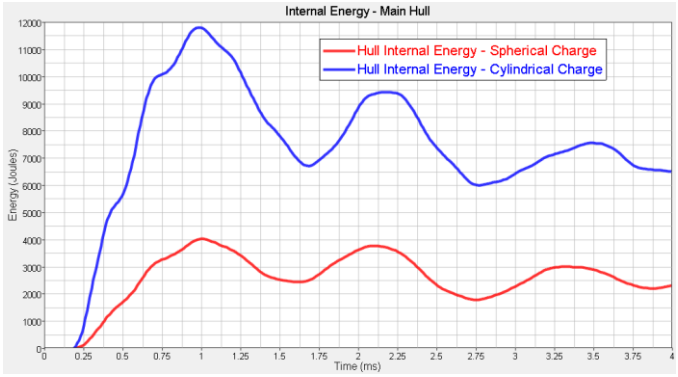

Figure 12: Free Air Burst – Cylindrical Charge, Hull Internal Energy

The cylindrical charge transmits significantly more energy to the vehicle. This effect is easily taken into account with FSI methods because the explosive charge is explicitly modeled. Whereas with a purely structural method, the explosive is assumed to be spherical and to account for a different explosive shapes the user has to scale the mass of the explosive using reference tables.

Figure 13 shows the pressure contour in the fluid elements at 0.2ms for both a cylindrical and spherical charge of CHARGE1 size. It can be seen that the pressure distribution is quite different with a cylindrical charge than with a spherical charge. This observation indicates that increasing the amount of explosive with a purely structural method may not capture the local deformation of the hull correctly near the charge.

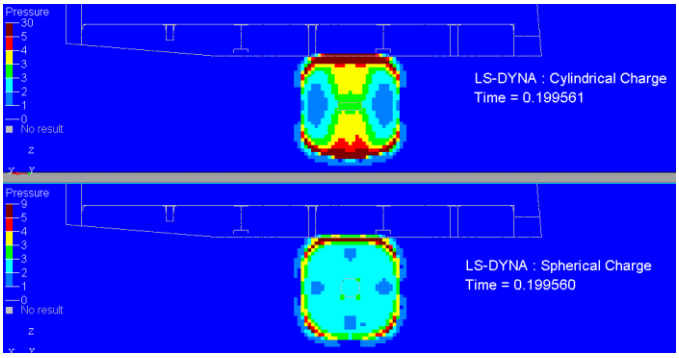

Figure 13: Free Air Burst –Pressure Profile, Cylindrical Charge (top), Spherical Charge (bottom)

SOIL DESCRIPTION

The type of the soil and the location of the explosive with respect to the ground surface can have a significant impact on the energy imparted from the explosive to the vehicle.

The free air blast model with a cylindrical charge of size CHARGE1 was modified to simulate a blast with an explosive charge buried 50.8mm below the ground surface. The soil composition is assumed to be dry sand. Figure 14 below shows the setup used.

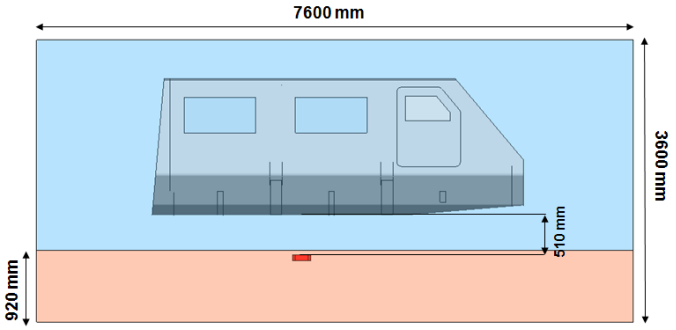

Figure 14: Soil Modelling – Setup

Figure 15 and Figure 16 show a comparison between FSI simulations with and without soil (air blast). The same mass and shape for the explosive charge is used for both simulations. The stress, deformation and internal energy of the hull are significantly higher in the model where the soil is considered. As expected, the soil tends to focus the blast energy toward the vehicle which results in larger deformations and increases the amount of energy imparted from the explosive to the vehicle.

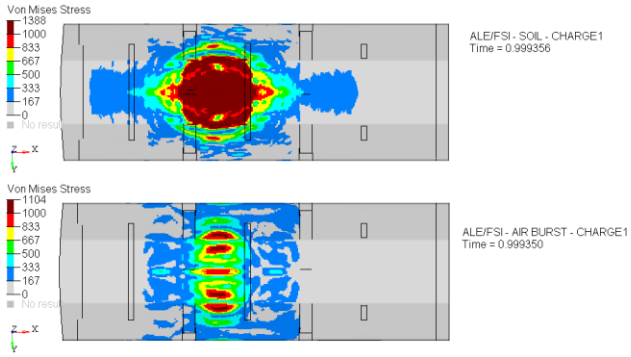

Figure 15: Hull Stress, Buried Charge (top), Air Burst (bottom)

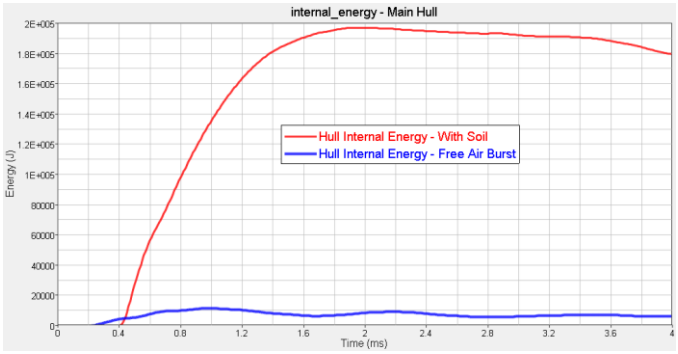

Figure 16: Soil Modelling, Hull Internal Energy

Similar conclusion was drawn when comparing a FSI simulation with soil and the structural simulation using *LOAD_BLAST which does not model the soil explicitly.

ALTERNATE BLAST SIMULATION USING SPH

Other methods like Smoothed-Particle Hydrodynamics (SPH) could be used to model the fluid instead of using an Eulerian formulation. SPH is commonly used to model fluid and structural parts where severe distortions are expected. Typical applications for SPH are bird impact and tank sloshing but it can also be used to simulate blast.

AIR BLAST – SPH

The effect of the free air burst of a spherical charge of size CHARGE1 under the vehicle was simulated with SPH. Figure 17 describes the model setup.

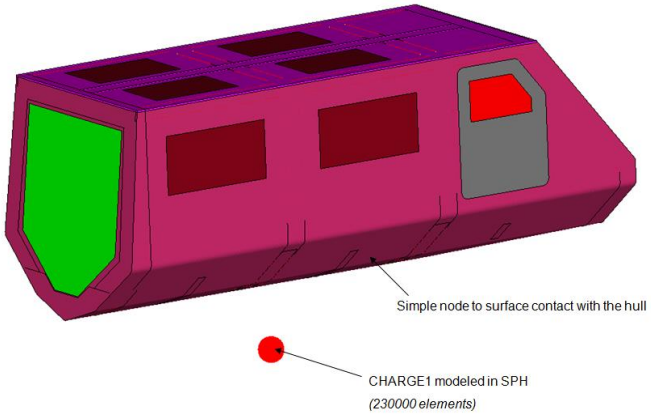

Figure 17: Free Air Burst – SPH Model Setup

In this example, the air surrounding the vehicle is not modeled due to significant cost in term of simulation time. The interaction between the particles and the vehicle is handled by an automatic node to surface contact. The default parameters were modified for the contact to behave properly: the bucket sort frequency was reduced and the initial stiffness of the contact was computed based on the master surface properties.

Figure 18 compares the stress distribution on the hull obtained with a structural method, FSI with an Eulerian formulation and using the SPH formulation. The stress distribution on the hull is similar for all 3 approaches. The magnitude of the stress on the hull is lower with the FSI methods than with the structural method.

The stress contour obtained with the SPH approach is not very continuous. This may be due to the fact that the air outside the vehicle is not modeled along with the way the particles are coupled to the structure. The particles are directly transferring loads to the vehicle where they are considered to be in contact and depending on the mesh density used for the particles, the loads may not be distributed evenly. In order to achieve meaningful results, a very large number of particles is necessary.

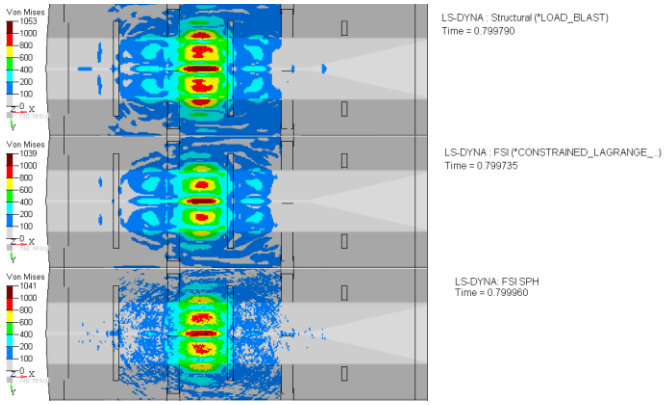

Figure 18: Free Air Burst – Hull Stress, Structural (top), FSI (mid), SPH (bottom)

Figure 19 compares the evolution of the internal energy of the hull for the different approaches. There is good agreement between the Eulerian and SPH approaches in LS-DYNA.

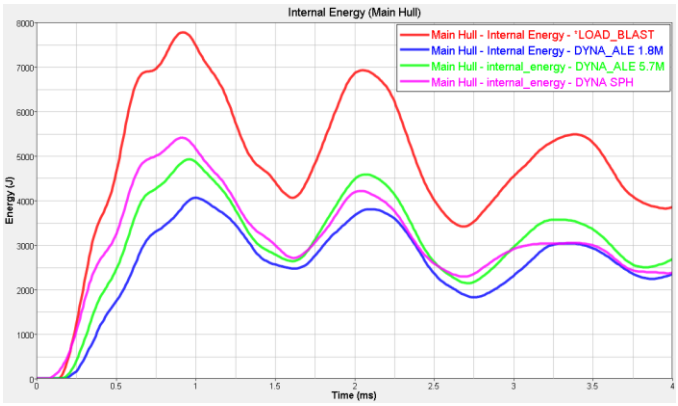

Figure 19: Free Air Burst – SPH Hull Internal Energy

BURIED EXPLOSIVE – SPH

The model developed for the ALE buried cylindrical explosive was used as a starting point and modified to create a similar setup for SPH. The Eulerian soil domain was replaced with SPH particles and Lagrangian elements. Additionally, the fluid structure couplings were replaced with a node to surface contact between the particles and the vehicle. Figure 20 shows the overall SPH model setup.

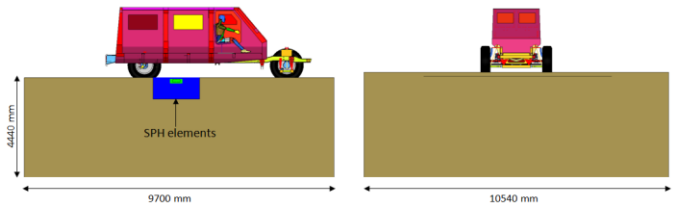

Figure 20: Buried Explosive – SPH Model Setup

The cost per cycle for SPH particles is larger than for traditional Lagrangian elements. In order to reduce the computation time only a portion of the soil was modeled with particles. Figure 21 shows the dimension of the domain modeled in SPH.

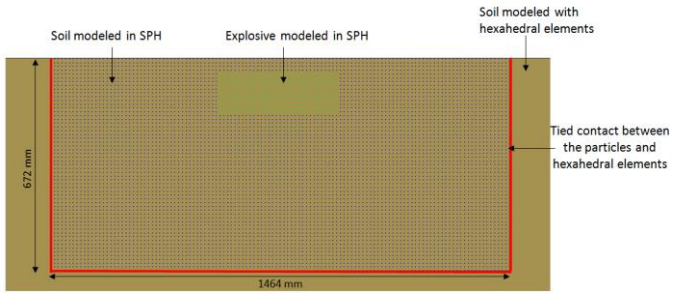

Figure 21: Buried Explosive – SPH Domain Dimensions

The model contains ~1.15 million particles (12mm pitch) and 450,000 hexahedral elements for the soil. The explosive charge is made up of 5,918 particles. The shape and mass of the explosive is identical to the one described in the buried ALE blast section of this paper. The same material model and equation of state are used for the soil and explosive.

Figure 22 shows the evolution of the deformation of the vehicle when the explosive and soil are modeled using SPH.

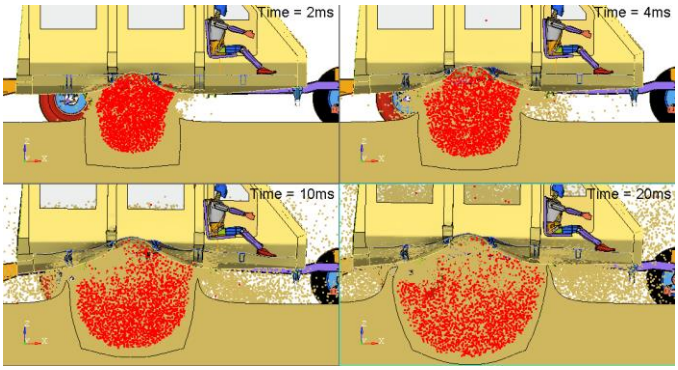

Figure 22: Buried explosive – SPH Deformation

Figure 23 shows the deformation comparison of the vehicle at 5ms when the explosive is modeled using SPH and ALE.

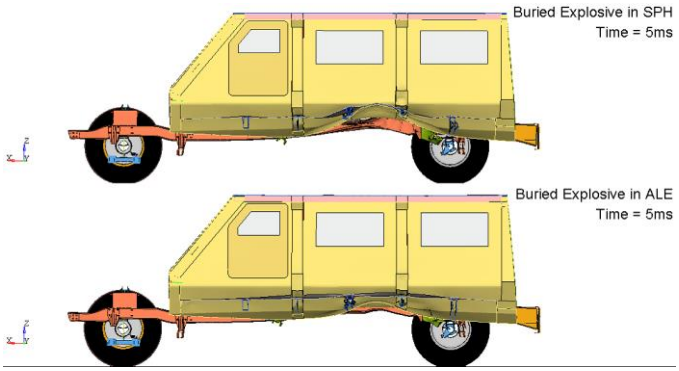

Figure 23: Buried Explosive – Deformation, SPH (top), ALE (bottom)

Figure 24 shows a comparison of the evolution of the deformation of the hull, in the area where the peak deflection is observed, as a function of time. The level of deformation observed is significantly larger in SPH than in ALE.

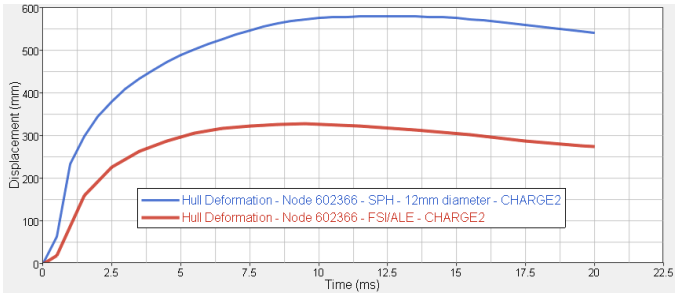

Figure 24: Buried Explosive – SPH vs ALE Peak Floor Deformation

The local deformation of the hull directly above the charge seems unrealistic in SPH. Those local distortions are generated by particles impacting the hull surface at very high speeds in the first milliseconds.

In order to improve the behavior of the contact, the particle diameter was reduced from 12mm to 8mm. The volume of the SPH domain was reduced to decrease the number of particles to 1.4 million.

Figure 25 shows a comparison of the deformation observed after 1.5ms with particles of 12mm and 8mm diameter. Increasing the number of particles improves the local deformation of the hull and decreases the overall level of deflection observed with the SPH approach.

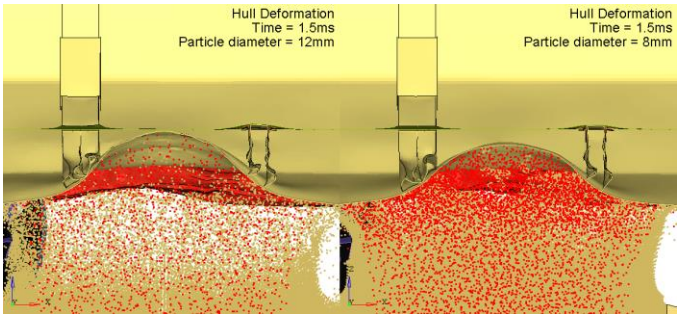

Figure 25: Buried Explosive – Influence of Particle Size on Vehicle Deformation

Figure 26 shows a comparison of the coupling force between the particles and the vehicle. Increasing the number of particles significantly decreased the peak load.

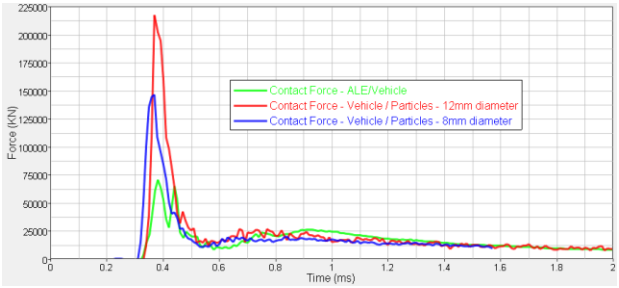

Figure 26: Buried Explosive – Influence of Particle Size on Contact Force

It is felt that modeling the air underneath the vehicle should improve the stability and the behavior of the contact, albeit at significant cost in term computational time; however, this has not been confirmed in this paper. Adding particles to model the air requires turning off the particle approximation between the different parts (explosive, soil, air) because of the difference in density and compressibility between the air and the soil/explosive. To handle the interaction between the different sets of particles, couplings (*DEFINE_SPH_TO_SPH_COUPLING) need to be defined. Several iterations were made on the coupling parameters, but no robust solution could be found.

To run the model with particles of 12mm in diameter for 20ms on 12 processors using LS-DYNA 971_r61 double precision required 83 hours for 27000 cycles. A similar ALE model setup only required 23 hours to complete for using the same hardware and solver version.

It should be noted that the internal energy of the hull is higher with the SPH approach than with the ALE approach, even when a very fine mesh is used for the ALE domain. A similar trend was observed in case of a buried explosive but on a larger scale. In order to determine which formulation is the most suited to model buried explosives, a systematic

correlation study to actual test data is deemed necessary, but is outside the scope of this paper.

COST EFFECTIVE BLAST SIMULATION

The vehicle model used for ALE buried explosive blast was utilized for this study. The explosive charge was sized to CHARGE2 (Appendix 1) to cause severe deformation of the hull, frame and chassis, and also impart significant kinetic energy to the vehicle.

Figure 27 shows the level of deformation of the hull and frame after 10ms. The hull deflects more than 300mm upward due to the explosive energy.

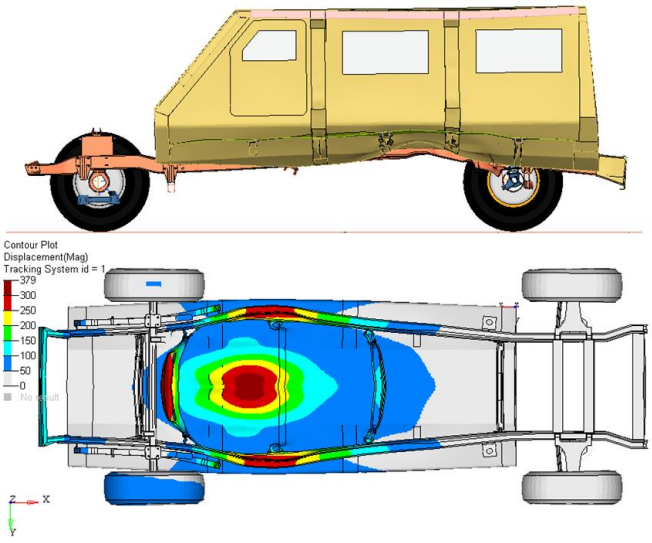

Figure 27: Full Blast Simulation Hull & Frame Deflection

Figure 28 shows the kinematics of the vehicle throughout the event. The total simulation time for this event was 2500ms. The energy transmitted from the explosive to the structure causes the vehicle to lift off the ground. The charge being off-center from the center of gravity of the vehicle causes a large rotation about the pitch axis. Gravity is active throughout the event and causes the vehicle to slam back to the ground.

An interesting phenomenon, not necessarily intuitive, should be noted here. While it is expected that a rear-of-cg blast location will rotate the vehicle in a counter-clockwise direction on the way up (210 to 610 ms), it may be observed that this counter-clockwise rotation continues even on the vehicle's way down (610 to 930 ms).

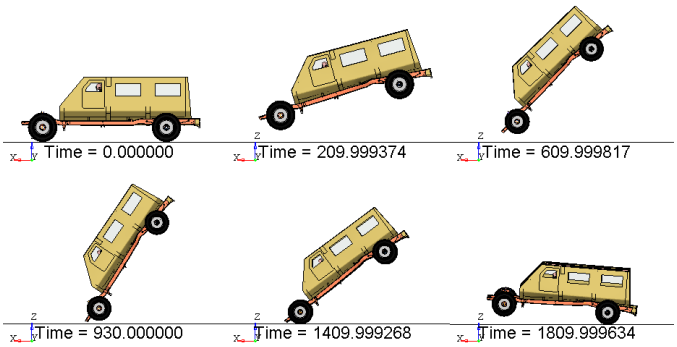

Figure 28: Full blast simulation – Vehicle Kinematics

The total duration of the simulation is very long for an explicit dynamic analysis. The run time to perform the analysis with all fluid elements, dummy, and fluid-structure coupling even for an event duration of 15ms using 12 processors is approximately 15 hours. Running the analysis for 2500ms while retaining all the fluid elements and a deformable vehicle is therefore not practical.

The following sections focus on some methods available in LS-DYNA to simulate the entire event within a reasonable time frame.

SMALL AND FULL RESTART OPTIONS

An explosion is a very dynamic event, when it occurs underneath a vehicle, and most of the energy transmitted from the explosive to the immediate surroundings occurs within the first few milliseconds.

Figure 29 shows the evolution of the coupling force between the fluid and the vehicle during the event. The coupling force is very high during the first 2 milliseconds and quickly decreases afterwards.

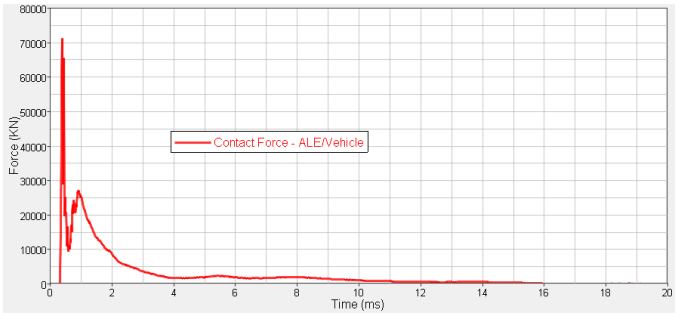

Figure 29: Full Blast Simulation – Coupling Force

The forces transmitted from the fluid to the structure are relatively low after 15ms. Removing the fluid elements and fluid-structure couplings from the analysis at this point should not significantly affect the results. On the other hand, removing those entities should be expected to dramatically

improve the speed of the simulation since there are on average about 8x more fluid than structural elements.

There are several ways to delete elements and couplings in LS-DYNA. In this study, we focused on two approaches.

SMALL RESTART OPTION

A full blast simulation could be run in two steps. The first step would have all the fluid elements and couplings active. These entities could be removed from the analysis in the second step.

The restart files (d3dump01.00xx) written at the end of the simulation of the full model are used as restart files in the command line when executing LS-DYNA. The small restart deck is used as input and the following command line can be used to restart the analysis:

v971_r50_double_mpp i=small_restart_deck.k r=d3dump01

Figure 30 shows an example of a small restart input deck. The commands *DELETE_PART and *DELETE_FSI are used to remove the fluid elements and couplings. The termination time, binary output frequency and time step scale factor can also be modified if desired.

```
*KEYWORD
*TITLE
LS-DYNA keyword deck by LS-PrePost
*CONTROL_TERMINATION
$$  ENDTIM    ENDCYC     DTMIN    ENDENG    ENDMAS
      2500
*CONTROL_TIMESTEP
$$  DTINIT    TSSFAC      ISDO    TSLIMT     DT2MS      LCTM     ERODE     MSIST
                 0.8
$$DATABASE_OPTION -- Control Cards for ASCII output
*DATABASE_ABSTAT
      0.50         3
*DATABASE_ELOUT
      0.50         3
*DATABASE_GLSTAT
      0.50         3
*DATABASE_MATSUM
      2.00         3
*DATABASE_RCFORC
      0.50         3
*DATABASE_BINARY_D3PLOT
$$ DT/CYCL      LCDT      BEAM     NPLTC
        40
         0
*DATABASE_EXTENT_BINARY
$$    NEIPH     NEIPS    MAXINT    STRFLG    SIGFLG    EPSFLG    RLTFLG    ENGFLG
                                         0         2         2         2         2
$$  CMPFLG    IEVERP    BEAMIP     DCOMP      SHGE     STSSZ    N3THDT    IALEMAT
                   1
$$ NINTSLD   PKP_SEN      SCLP                MSSCL     THERM
*DELETE_PART
       100       101       102       103       104
*DELETE_FSI
       102       103
*END
```

Figure 30: Full Blast Simulation – Restart Small Input Deck

To assess the benefit of deleting the fluid elements and couplings from the simulation once most of the blast energy has been transmitted two simulations were performed. In the first simulation, the fluid elements and couplings were kept active, while in the other, they were removed from the analysis after 15ms with the small restart option. Each simulation was run for a total of 75ms.

The simulations were run on the same platform with the same number of processors (12) and version of LS-DYNA (971_r50 double precision MPP). It required 59 hours to run the full FSI simulation for 60ms (from 15ms to 75ms) with the small restart option, it required only 5 hours. The small restart option allows a speed up of almost 12x compared to the full FSI simulation.

Figure 31 and Figure 32 show comparisons of the displacement and velocity of the hull at 75ms respectively. The results are similar overall with the vehicle approximately 30mm higher in the full FSI model than where the fluid and couplings were removed after 15ms. This difference could be reduced by retaining the fluid elements longer before removal. The dummy kinematics shown in Figure 33 are also similar for the two simulations.

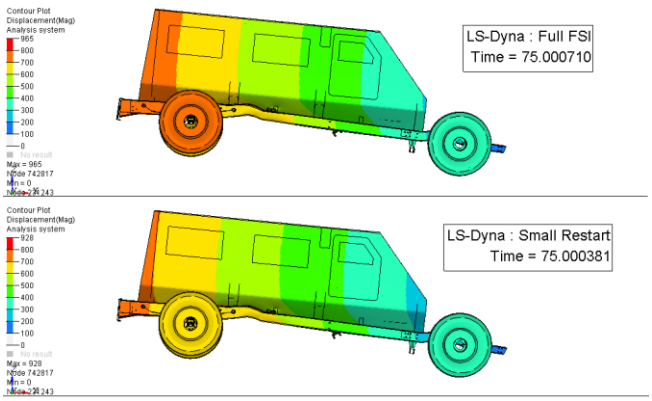

Figure 31: Full FSI vs Restart – Displacement Plot, Full restart (top), Small restart (bottom)

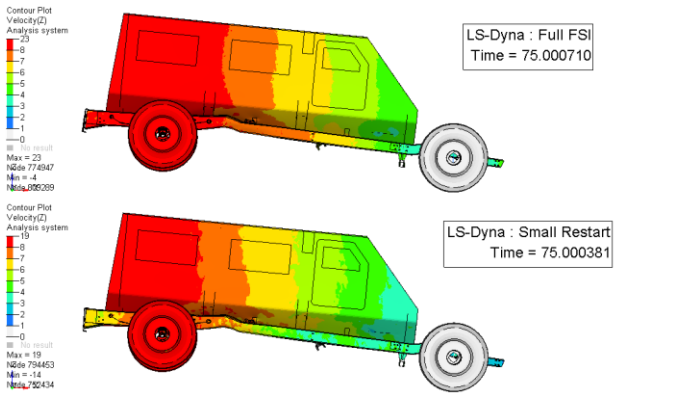

Figure 32: Full FSI vs Restart – Velocity Plot, Full restart (top), Small restart (bottom)

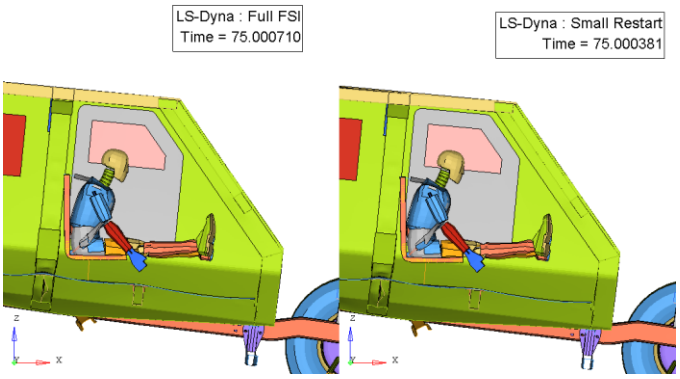

Figure 33: Full FSI vs Restart – Dummy kinematics, Full restart (left), Small restart (right)

FULL RESTART OPTION

The concept for a full restart is very similar to that described for the small restart. The idea is to delete the fluid elements and couplings once the force between the fluid and the structure is deemed small enough.

With the full restart option the fluid components, couplings and all keywords related to the fluid elements are deleted from the full input deck. The new input deck created contains only the vehicle, dummy and the rigid ground.

To initialize the model with the results from the full simulation the keyword *STRESS_INITIALIZATION needs to be invoked. This keyword allows initializing all the parts in the models using the data from the d3full01. The following command line is used to do a full restart of the analysis:

v971_r61_double_mpp i=full_restart_deck.k n=d3full01

It should be noted that some keywords are not currently compatible with the full restart option, for example *CONTACT_AUTOMATIC_GENERAL cannot be used if a full restart needs to be performed. Also, a bug in the initialization of the velocities of nodal rigid bodies when performing a full restart was reported to LSTC. The velocities of the nodes belonging to nodal rigid bodies that were not distributed to processor 0 in MPP were not initialized with the full restart (initial velocity = 0). The bug was fixed by LSTC in a later beta version.

There are 3 major advantages of performing a full restart over a small restart:

1. Scalability - With the small restart option, LS-DYNA performs the domain decomposition on the full model with all the ALE elements and couplings. The domain decomposition is not modified with the small restart option. This could adversely affect the scalability because the load may not be balanced evenly across all CPUs. With the full restart option, the domain decomposition is performed on the new input deck generated which should improve the scalability.
2. Time Step Treatment (mass scaling) - Using mass scaling on Eulerian or Arbitrary Lagrangian Eulerian simulation is generally not recommended. A small time step scale factor is also recommended (0.7 or lower). With the small restart option, the time step scale factor can be changed but mass scaling cannot be activated. With the full restart option, both options are available.
3. Binary Output File Size - The file size of each d3plot for the full model is about 600Mb. With the small restart option, even though the fluid elements are deleted, the size of the d3plot does not change. With the full restart option each d3plot contains only the vehicle, dummy, and the rigid ground. The size of a d3plot is therefore about 70Mb.

DEFORMABLE TO RIGID

The *DEFORMABLE_TO_RIGID_AUTOMATIC card in LS-DYNA allows switching parts from deformable to rigid and rigid to deformable based on the force value in a specific contact or rigid wall. The switching behavior can be tailored with additional timing controls on the card as required.

The blast energy causes the vehicle to lift-off the ground for long durations before slamming back down. When the vehicle is in lift-off or freefall phase, gravity is the only external load active. The deformation of the hull and chassis during these phases is not expected to be significant. The simulation time could be reduced if the hull and chassis were switched to rigid when the vehicle is not in contact with the ground.

In this study a separate surface to surface contact was defined for the contact between the rigid ground and the vehicle and 2 *DEFORMABLE_TO_RIGID_AUTOMATIC cards were defined:

- The first card allows switching the chassis and hull from deformable to rigid. The CODE=2 is used and allows activating the switch when the contact force between the ground and the vehicle is null. TIME 1 is set to 100ms so that no switch occurs during the explosion phase. TIME 3 is set to 1ms in order to avoid excessive switching from deformable to rigid because of contact chartering.
- The second card allows switching the chassis and hull from rigid to deformable. The CODE=4 is used and allows activating the switch when the contact force between the ground and the vehicle is non-zero.

The two cards are paired by their switch number. The first switch (from deformable to rigid) is the master switch. The master switch will be activated before the slave switch.

Pairing allows multiple switches to take place when the contact condition is active or inactive several times throughout the analysis.

Figure 34 shows the parts that are switched to rigid when the contact force is null. The seat, restraint system, dummy, and suspension are considered deformable throughout the event.

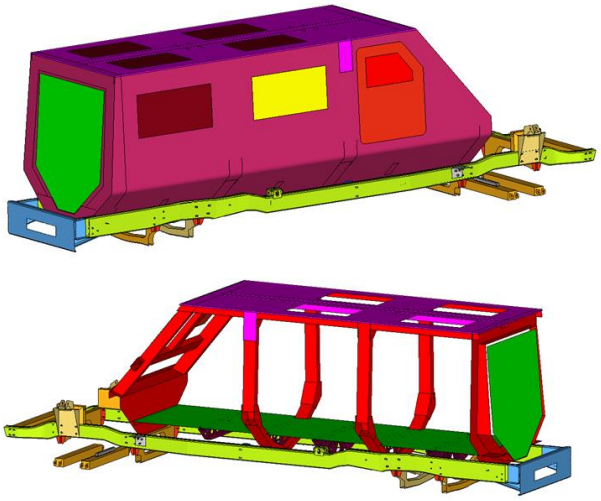

Figure 34: Full Blast Simulation – Rigid to Deformable, parts that are switched to rigid when contact force is null

Figure 35 shows the evolution of the time step and contact force between the vehicle/ground. When the contact force is null, part of the vehicle become rigid and the time step increases (the time step was controlled by an element of the chassis). When the contact force is non-zero, a portion of the vehicle switches from rigid to deformable and the time step decreases.

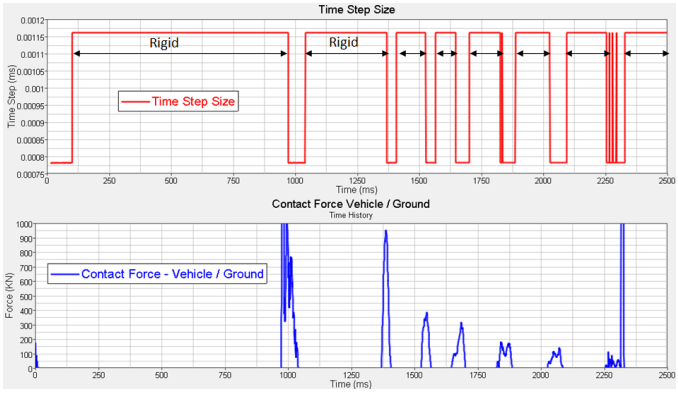

Figure 35: Full Blast Simulation – Rigid to Deformable Time Step Size

Figure 36 shows a comparison of the displacement between a simulation using the deformable to rigid option and the other with a fully deformable vehicle. The results are very similar.

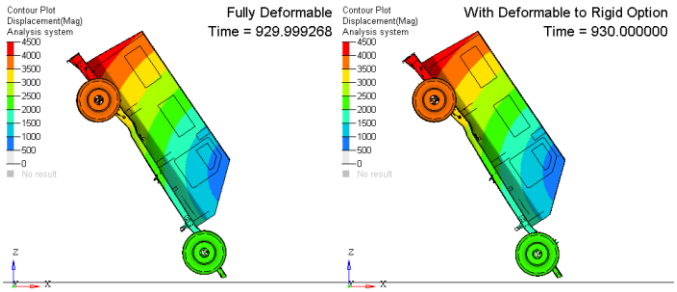

Figure 36: Full Blast Simulation – Displacement Plot, Fully Deformable (left), Rigid to Deformable option (right)

Using the automatic deformable to rigid options yields a variable gain in term of simulation time. If the vehicle is always in contact with the ground there is no gain in simulation time. If the lift-off and free fall phases last for a long period, then the gain could be significant. In this study, a reduction of 40% of the simulation time was observed.

Some potential issues regarding the automatic rigid to deformable option have been reported to LSTC: not all nodal rigid bodies appear to be merged correctly in MPP; when the parts switch from deformable to rigid some rigid bodies appear to have null inertias. These issues are currently under review by LSTC Development team.

Several keywords can be used in conjunction with the deformable to rigid option in order to optimize the domain decomposition. The idea is to distribute the elements belonging to the parts that are deformable throughout the analysis evenly across all CPUs. For example, the keyword *CONTROL_MPP_DECOMPOSITION_PARTSET_DISTRIBUTE could be used.

SIMULATION TIME

Combining various restart options with automatic deformable to rigid control was studied for reduction in simulation time. Table 1 summarizes the run time achieved for 4 different study configurations:

1. FSI with small restart and a fully deformable vehicle.
2. FSI with small restart including the automatic rigid to deformable option.
3. FSI with full restart including the automatic rigid to deformable option.
4. Scaled CONWEP (*LOAD_BLAST) with automatic rigid to deformable option.

Study	MPP Version	Run Time: 0ms to 10ms	Run Time: 10ms to 2000ms	Total Simulation Time
1	971_r50 double	8 hours	163 hours	171 hours
2	971_r50 double	9 hours	94 hours	103 hours
3	971_r61 double	15 hours	43.5 hours	58.5 hours
4	971_r61 double	0.5 hours	41 hours	41.5 hours

Table 1: Comparison of Simulations

The fluid elements (air, soil, explosive) are deleted after 10ms. A rigid material is used in this study to model the ground on which the vehicle lands. A compliant ground could be used instead if deemed necessary or more accurate.

All models were run on similar hardware:

- Operating System: Linux64
- Processors: 2 Intel Xeon X5650 at 2.67 GHz (6 cores per processor)
- Memory: 32Gb

CONCLUSIONS

- When an explosion occurs underneath an armoured vehicle, severe deformation of the hull and chassis can occur. Simulating the entire event such as deformation of the floor, blast-off, gravity flight, and slam down with traditional methods is inefficient, as calculation times may exceed several days or even weeks.
- The current method of choice to simulate the effect of an explosive buried underground on a vehicle is a fluid-structure interaction with the environment modelled with an Eulerian formulation (explosive, ground, air). This method is more expensive and involved than purely structural methods (pressure loads applied on the vehicle surface), but allows taking into account the effect of the shape of the charge and stiffness of the soil on the energy transmitted to the vehicle.
- The SPH formulation can alternatively be used to simulate buried explosives, however SPH is observed to be more costly than an equivalent ALE approach. Also, results obtained with this method were significantly different that those obtained with the Eulerian formulation.
- In this study, the results with the SPH approach, and to a lesser extent with the Eulerian formulation, were found to be dependent on the mesh density and the numerical parameters used to couple the environment (soil, explosive, air) to the vehicle. In order to determine which formulation is the most appropriate to simulate the effect of an underbody blast, a correlation to actual test data is deemed necessary.
- The SPH method is equally challenging to execute as the ALE formulation, especially as it pertains to the load transfer at the underbody interface, with various parameters that need tuning in order to produce reasonable results. These findings appear contrary to claims made by software vendors in current literature about SPH and Eulerian-to-SPH methodologies.
- Three methods are proposed to reduce the simulation time for a given blast event. The first two (small and full restart) involve removing the fluid elements and couplings once the loads transmitted from the fluid to the structure are deemed small enough. When the fluid elements and couplings are removed from the analysis the complete 2000ms simulation is estimated to be more than 10 times faster.
- The full restart option is more efficient than the small restart option and allows more control of changes to the model upon restart. Another method is to switch part of the vehicle to rigid (hull, chassis) when it is not in contact with the ground during the gravity-flight and free-fall stages. In this study, an additional reduction of 40% of calculation time was observed by adopting this method.

REFERENCES

[1] Thyagarajan, R. (2000) “End-to-end System level M&S tool for Underbody Blast Events”. 27th Army Science Conference, Army Technology Showcase, FL, Nov 29 – Dec 2. DTIC Report # AD A550921

[2] J. Jablonski, P. Carlucci, R. Thyagarajan, B. Nandi, and J. Arata (2012). “Simulating Underbelly Blast Events using Abaqus/Explicit – CEL”. 2012 SIMULIA Customer Conference, DTIC Report # AD A571166

[3] Livermore Software Technology Corporation, LS-DYNA Keyword User’s Manual (2012) Version 971 R6.1.0

[4] Altair Engineering, RADIOSS Keyword User’s Manual (2012) Release 12.0.110

[5] Richard Weed, Christopher Moore & Ravi Thyagarajan (2011). “Implementation of ERDC HEP Geo-material Model in CTH and Application to Buried Explosives Simulations”. Numerical Methods for Blast Effects, 82nd Shock and Vibration Symposium, Baltimore, MD, Oct 31 - Nov 3. DTIC Report # AD A551236

[6] Richard Weed, Christopher Moore, Ravi Thyagarajan (2013). “Enhancements and Analysis of CTH Software for Underbody Blast”. DTIC Report # AD A571176, March.

[7] Thyagarajan, R., Kosarek, P., Parthasarathy, M., & Santini, J. (2013) “Development of Computationally Efficient Models in LS-DYNA for Full Underbody Blast Events”. TARDEC Report #24224.

[8] Kulkarni, K., Ramalingam, J., and Thyagarajan, R. (2014). "Assessment of the Accuracy of Certain Reduced Order Models used in the Prediction of Occupant Injury during Under-Body Blast

Events," SAE Int. J. Trans. Safety 2(2):2014, doi:10.4271/2014-01-0752.

[9] Kulkarni, K.B., Ramalingam, J., and Thyagarajan, R. (2013). "Evaluating the Effectiveness of Various Blast Loading Descriptors as Occupant Injury Predictors for Underbody Blast Events". NDIA Ground Vehicle Systems Engineering and Technology Symposium (GVSETS) Modeling & Simulation, Testing and Validation (MSTV) Mini-Symposium August 21-22, Troy, Michigan. DTIC Report #: AD A590537

[10] Li, L., Stowe, N., Vlahopoulos, N., Mohammad, S., Barker, C., Thyagarajan, R. (2013). "Utilization of Fast Running Models in Buried Blast Simulations of Ground Vehicles for Significant Computational Efficiency". NDIA Ground Vehicle Systems Engineering and Technology Symposium (GVSETS) Modeling & Simulation, Testing and Validation (MSTV) Mini-Symposium August 21-22, Troy, Michigan, DTIC Report # AD A590114

[11] Jaisankar Ramalingam, Sherri Chandra, Ravi Thyagarajan (2013, 2014). "Reduced Order Modeling for Rapid Simulations of Blast and Rollover Events of a Ground Vehicle and its Occupants Using Rigid Body Dynamic Models". DTIC Report # AD A585048. Also published in the 2014 NDIA Ground Vehicle Systems Engineering and Technology Symposium (GVSETS) Modeling & Simulation, Testing and Validation (MSTV) Mini-Symposium August 12-14, Novi, Michigan, DTIC Report # AD A609195

[12] Risa Scherer (2010), "Vehicle and Crash-Dummy Response to an Underbelly Blast Event", 54th Stapp Conference (Oral Only), November 3-5, Scottsdale, AZ.

[13] Daniel Dooge, Ramesh Dwarampudi, Grant Schaffner, Adam Miller, Ravi Thyagarajan, Madanmohan Vunnam & Venkatesh Babu (2011). "Evolution of Occupant Survivability Simulation Framework Using FEM-SPH Coupling". 2011 NDIA Ground Vehicle Systems Engineering and Technology Symposium (GVSETS), Dearborn, MI, Aug 9-11. DTIC Report # ADA547566

[14] K. Williams, et. al, (2002), "Validation of a Loading Model for Simulating Blast Mine Effects on Armoured Vehicles", 7th International LS-DYNA Users Conference.

[15] Thyagarajan, R., Ramalingam, J., and Kulkarni, K.B., (2014). "Comparing the Use of Dynamic Response Index (DRI) and Lumbar Load as Relevant Spinal Injury Metrics". ARL Workshop on Numerical Analysis of Human and Surrogate Response to Accelerative Loading, Jan 7-9, Aberdeen, MD. DTIC Report # AD A591409

[16] W Jiang, N Vlahopoulos, M Castanier, R Thyagarajan, S Mohammad, (2014). "Reducing Structural Weight and Increasing Protection in Simple Structures Subjected to Blast Loads". NDIA Ground Vehicle Systems Engineering and Technology Symposium (GVSETS) Modeling & Simulation, Testing and Validation (MSTV) Mini-Symposium August 12-14, Novi, Michigan, DTIC Report # AD A612781

[17] Jai Ramalingam and Ravi Thyagarajan, "Effect of Reclining Seat Position on Blast Mitigation", Armor/Anti-Armor Threat Coordinating Group, NGIC Meeting# 2784, Charlottesville, VA, July 24-26, 2012 DTIC Report # AD B387221

[18] Kingery, C., and Bulmarsh, G. (1984) "Airblast parameters from TNT Spherical Air Burst and Hemispherical Surface Burst," ARBRL-TR-02555

ACKNOWLEDGMENTS

The authors would like to thank the Underbody Blast Modeling/Methodology (UBM) program (Program Manager: Mr. Craig Barker), managed by the U.S. Army Research Laboratory's Survivability/Lethality Analysis directorate (ARL/SLAD) and the U.S. Army Test and Evaluation Command (ATEC), for the funding provided which made this project possible. This material is based on Research and Development (R&D) work supported by the U.S. Army Tank-automotive and Armaments Command (TACOM) Life Cycle Command under Contract No. W56HZV-08-C-0236, through a subcontract with Mississippi State University (MSU), and was performed for the Simulation-Based Reliability and Safety (SimBRS) research program. Any opinions, finding and conclusions or recommendations in this paper are those of the author(s) and do not necessarily reflect the views of the U.S. Army TACOM Life Cycle Command.

DISCLAIMER

Reference herein to any specific commercial company, product, process, or service by trade name, trademark, manufacturer, or otherwise, does not necessarily constitute or imply its endorsement, recommendation, or favoring by the United States Government or the Department of the Army (DoA). The opinions of the authors expressed herein do not necessarily state or reflect those of the United States Government or the Department of the Army (DoA), and shall not be used for advertising or product endorsement purposes.

APPENDIX 1: Charge sizes used in the simulations

ID	Size
CHARGE1	Typical blast mine used for benchmarking blast simulations [13,14]
CHARGE2	2.5 times CHARGE1